International Journal of Automotive Technology, Vol. 6, No. 2, pp. 191–196 (2005)

1229–9138/2005/020–13

EFFECTS OF FORMING PROCESS ON SEALING PERFORMANCE OF FULL-BEAD OF MLS GASKET: FINITE ELEMENT ANALYSIS APPROACH

S.-S. CHO[1)*], B. K. HAN[1)], H. CHANG[2)] and B. K. KIM[3)]

[1)]Department of Mechanical & System Design Engineering, Hongik University, Seoul 121-791, Korea
[2)]Hyundai Motor Company, 772-1 Jangduk-dong, Hwaseong-si, Gyeonggi 445-706, Korea
[3)]Department of Mechanical & Automotive Engineering, Inje University, Gyeongnam 621-749, Korea

(Received 6 November 2003; Revised 23 April 2004)

ABSTRACT–A full-bead of multi-layer-steel (MLS) engine head gasket is used to seal the combustion gas. Finite element analyses were conducted to assess the dependence of the sealing performance of full-bead on the forming process consisting of embossing and flatting operations. It is demonstrated that the sealing performance is enhanced with more severe deformation of the bead plate during the embossing, i.e., with the increase in the punching depth, the punch height, the punch width and the friction coefficient of the bead plate against the punch and die, and with the decrease in the width of die cavity. Meanwhile, the flatting process that is employed to adjust the height of the embossed full-bead has no influence on the sealing performance.

KEY WORDS : MLS engine head gasket, Full-bead, Sealing, Finite element analysis, Forming, Load-bead height curve

1. INTRODUCTION

Cylinder head gaskets, fastened between the cylinder head and the cylinder block with bolts, are used to seal the combustion gas, lubrication oil and coolant. Various head gaskets such as asbestos gaskets, composite gaskets and metal gaskets have been introduced in the market. Asbestos gaskets are out of use in modern engines because they are harmful to human health and exhibit insufficient performance. Composite gaskets that were developed to overcome the shortcomings of asbestos gaskets have been being replaced with metal gaskets because modern engines that are characterized as simultaneous higher output and lighter weight requires the head gasket to correspond to a narrow land between cylinder bores, to minimize cylinder bore distortion and to decrease crevice volume as well as to ensure high durability and reliability (Yamaguchi *et al.*, 1998).

Metal head gaskets are classified into single plate and multi-layer plates. Multi-layer steel (MLS) gaskets are further classified into grommet and bead types. The grommet types for large heavy-duty diesel engines seal the combustion gas with a grommet or a combination of grommet and wire ring whereas the bead types for general automotive engines use high compressive recovery of the bead.

Figure 1 shows the basic sealing structure of MLS bead type gaskets. It is made of cold-rolled stainless steel thin plate with thin elastomer coatings for micro sealing on both sides. Full-beads seal the combustion gas while half-beads seal lubrication oil and coolant. Sealing function of the beads is accomplished with the elastic compressive energy stored in the beads during the fastening operation. When the combustion pressure lifts off the cylinder head, the stored energy recovers the shape of the compressed bead so that the bead keeps in contact with the surface of head or block. A stopper, which is a relatively thick portion around the engine bore, serves as the primary static sealing area. It also reduces the gap movement in the bead area by pretensioning the engine parts, and enhances durability of the bead by limiting the bead deflection (Novak *et al.*, 1998). A shim, which is a separate narrow sheet contacting the full-bead, prevents leakage owing to surface porosity and diminishes wear in the bead area.

The compressive force acting on the beads varies periodically during the engine operation because the combustion pressure increases the sealing gap and thus weakens the compressive force exerted by the fastening bolts. Hence, the bead must maintain the sealing function even for the largest sealing gap, and also possess sufficient fatigue crack resistance. Both the sealing

*Corresponding author. e-mail: sscho@hongik.ac.kr

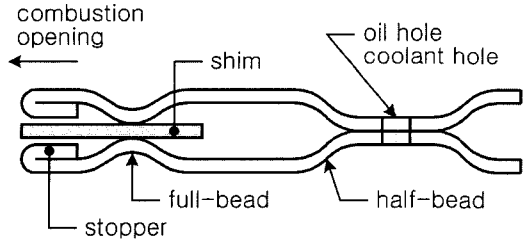

Figure 1. Basic structure of MLS bead type gasket.

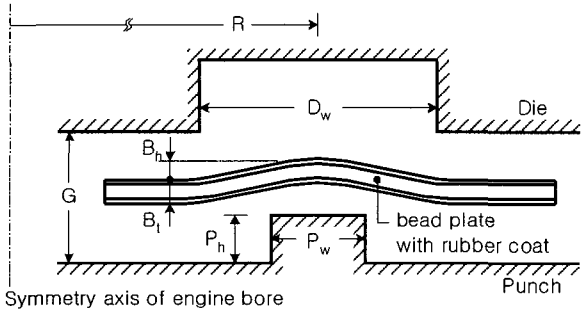

Figure 2. Schematic representation of full-bead, embossing punch and die with nomenclature.

performance and the fatigue crack resistance must be assured in the development stage. However, experimental assessment is very difficult and time-consuming, and provides only qualitative estimation because the head gaskets are used in difficult-to-access location and complicated circumstances (Ishigaki *et al.*, 1993). Therefore, various efforts have been made recently to develop CAE approaches based on the finite element methods (Harland *et al.*, 1993; Herbert *et al.*, 1998; Popielas *et al.*, 2000).

This paper, a partial result of development of methodology for computer-aided assessment of MLS bead type gaskets, presents a finite element model for assessment of the sealing performance of full-bead formed on rubber pre-coated plates and discusses the dependence of the sealing performance on the forming parameters.

2. FINITE ELEMENT MODEL AND ANALYSIS PROCEDURE

A finite element model has been developed to simulate the forming process of full-bead and then assess its sealing performance. The full-bead is formed on SUS301 cold-rolled thin plate with NBR (nitril butadiene rubber) coatings on both sides. The forming process consists of the embossing operation to form the full-bead and the flatting operation to adjust the height of the embossed full-bead. Figure 2 shows the schematic representation of the full-bead and a set of punch and die for the embossing

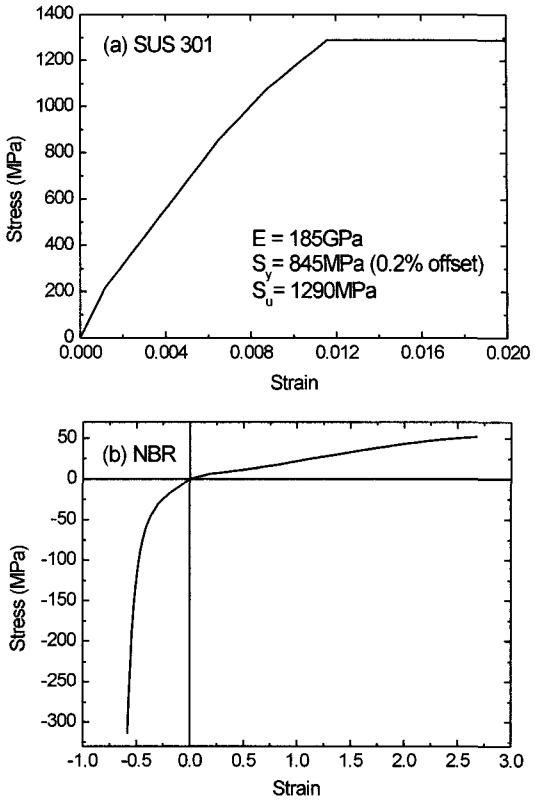

Figure 3. Stress-strain curves for (a) SUS301 thin plate and (b) NBR.

with nomenclatures.

The mesh was constructed for the annular region of the gasket including the full-bead around the engine bore (refer to Figure 2). The bead plate consists of 0.2 mm thick SUS plate and two layers of 0.025 mm thick coatings. The width of the annular plate was 5.7 mm. The mesh was constructed with 4-node axisymmetric hybrid elements of 25 μm × 25 μm. However, the elements of 6.25 μm × 6.25 μm were used for the region where the bead plate is in contact with the corners of the dies. The embossing punch and die, and the flatting dies for the simulation of forming process, and the cylinder head and block for the simulation of fastening and the head lift-off were modeled as rigid bodies. Corner radius of the embossing dies was assumed to be 50 μm.

Figure 3 shows stress-strain curves for the SUS301 thin plate and the NBR coating obtained from uniaxial tensile and compression tests. With the data shown in Figure 3, the SUS plate was assumed as a elasto-plastic material with an elastic modulus of 185 GPa, a 0.2% offset yield strength of 845 MPa, and an ultimate tensile strength of 1.29 GPa, while the NBR was assumed as a hyper-elastic material with the strain energy potential given as:

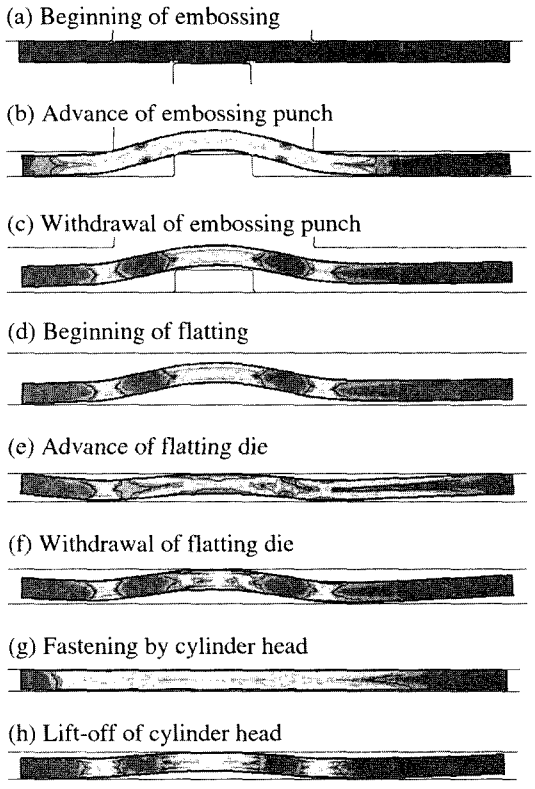

Figure 4. Finite element analysis procedure.

$$U = \sum_{i=1}^{2} C_{i0}(\bar{I}_1 - 3)^i \quad (1)$$

where $C_{10} = 7.24$ MPa and $C_{20} = 8.9$ kPa, and $\bar{I}_1$ is the first deviatoric strain invariant. Sliding friction tests of the NBR-coated plate against the steel block gave the friction coefficient in the range from 0.1 to 0.3. Hence, the friction coefficient of the plate against all the rigid bodies in the model was set equal to 0.2.

The simulation was conducted with a commercial finite element code ABAQUS. A quasi-static incremental solution technique was employed with nonlinear geometry analysis scheme. No boundary condition was specified for the mesh as for the real gasket. That is, the rigid body motion in the radial direction is self-constrained since the model is axisymmetric. The gravitational force is included to prohibit the rigid body motion in the axial direction. The motion of the forming dies was displacement-controlled while that of the head was force-controlled in order to mimic the real situation. The investigation intended to reveal the dependence of the sealing performance on the embossing parameters such as the punching depth, the punch height, the punch width, the width of die cavity, and the friction coefficient, and the dependence on the flatting operation.

Figure 4 shows the analysis procedure. The analysis starts with the forming simulation of full-bead. The bead plate is positioned between a set of the embossing punch and die (Figure 4(a)). The embossing punch advances (Figure 4(b)) and then withdraws (Figure 4(c)) to form a full-bead. Since the embossed full-bead is taller than the height specified in the design, the flatting operation follows to adjust the height to the design value. The embossed full-bead is positioned between two flatting dies (Figure 4(d)), and then it is compressed (Figure 4(e)) and released (Figure 4(f)) by the upper flatting die. The stroke of the embossing and the flatting were set equal to the values used in the manufacture of the gasket. After the forming is completed, the full-bead is fastened between the cylinder head and the block. The fastening is simulated by moving down the head against the block until the fastening load reaches a specified value (Figure 4(g)). After the installation, the lift-off of the head due to the combustion pressure is simulated. The head is moved upward to allow the fastened full-bead to recover its shape (Figure 4(h)). During the up-and-down movement (Figure 4(g)-(h)), the load-bead height curve that shows the relationship between the sealing force and the head-block sealing gap is obtained. The up-and-down movement is repeated until the curve is stabilized. The stabilized curve is used to estimate the dynamic sealing performance of the full-bead.

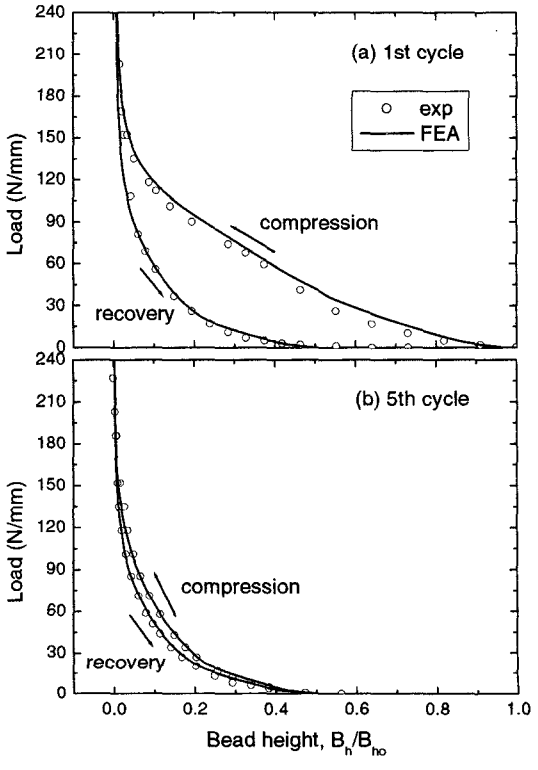

Figure 5. Load-bead height curve.

3. RESULTS AND DISCUSSION

3.1. Model Verification

Figure 5 shows the load-bead height curves during the first and the fifth cycles of the compression and the recovery. The load is the reaction force of full-bead of unit circumferential length. The head height B_h is normalized with the initial height B_{ho}, i.e., the height before the fastening. The compression curve for the first cycle corresponds to the fastening of the full-bead, and that for the remaining cycles corresponds to the downward movement of the cylinder head with the decrease in the combustion pressure during the engine operation. The recovery curve corresponds to the shape recovery of the compressed full-bead during the lift-off of the head. The curve for the first cycle differs significantly from that for the fifth cycle because of the plastic deformation of full-bead during a few early cycles. Figure 4 also shows the experimental data, demonstrating excellent agreement between the analysis and the test results. Hence, it is claimed that the model predicts the behavior of full-bead accurately.

3.2. Assessment of Forming Process

The influence of the forming process on the sealing performance is examined with the recovery curve at the fifth cycle. During the engine operation the maximum combustion pressure is fixed so that the sealing gap varies in a fixed range. Hence, the sealing performance is assessed with the criterion that the full-bead possesses better sealing performance when the sealing force, i.e., the reaction force of full-bead is higher for a given range of the sealing gap.

Figure 6 shows the effect of the punching depth on the sealing performance. The punching depth means the penetration depth of the embossing punch into the die cavity at the end of the punching stroke, and it is represented by the punch-die gap at the end of the stroke subtracted with the thickness of the bead plate, G-B_t (refer to Figure 2). When the punching depth is higher, the curve decreases more slowly. Slower decrease of the curve means that the sealing force is stronger at the given sealing gap. Hence, the increase in the punching depth improves the sealing performance.

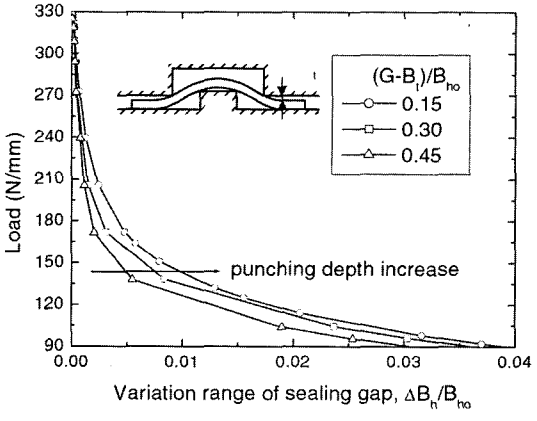

Figure 6. Effect of punching depth.

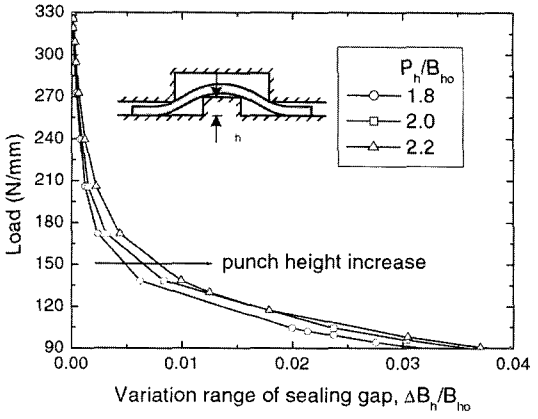

Figure 7. Effect of punch height.

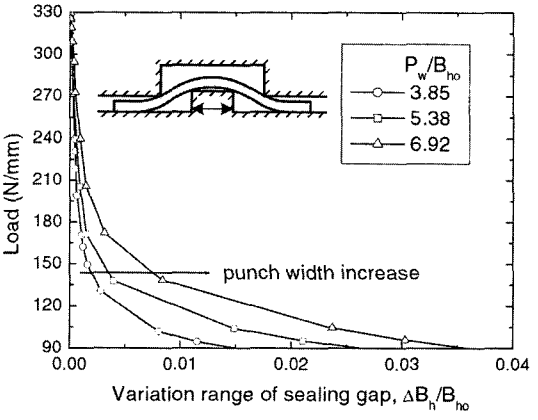

Figure 8. Effect of punch width.

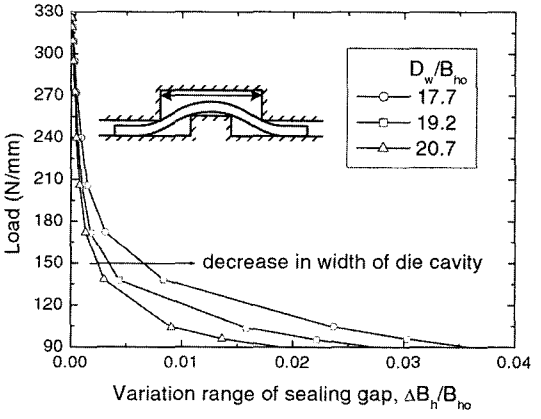

Figure 9. Effect of width of die cavity.

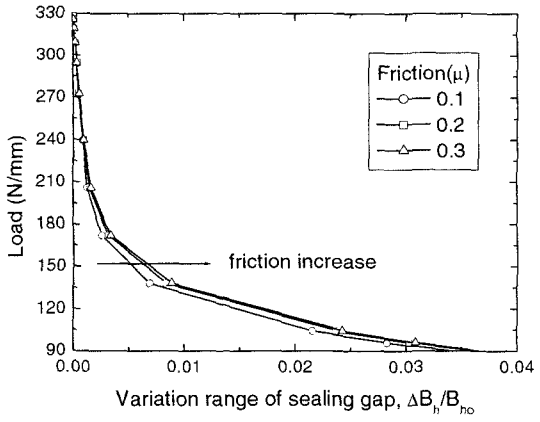

Figure 10. Effect of friction coefficient.

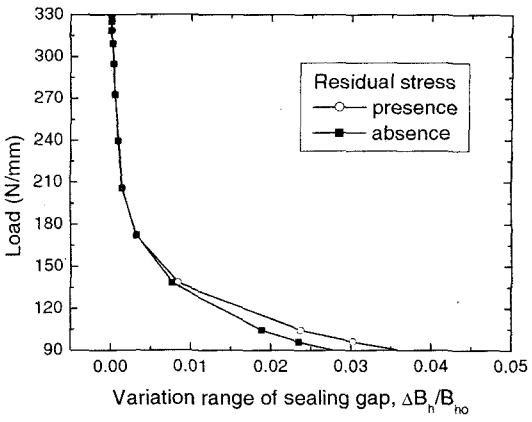

Figure 12. Effect of residual stresses.

Figures 7~10 show the effect of the punch height P_h, the punch width P_w, the width of die cavity D_w, and the friction coefficient μ of the bead plate against the punch and the die, respectively. The curve decreases more slowly for taller and wider punch, narrower die cavity, and higher friction coefficient.

With the increase in the punching depth, the punch height, the punch width and the friction coefficient and with the decrease in the width of die cavity, the bending angle of the bead plate contacting the corner of die increases, and thus more severe deformation occurs in the bead plate. Hence, it is concluded that the sealing performance is enhanced with the selection of embossing parameters producing larger deformation.

Figure 11 shows the effect of flatting operation. The flatting operation is conducted in one case whereas not in the other case after the full-bead is embossed under an identical condition. Since no difference is observed, it is claimed that the flatting operation has no influence on the sealing performance.

Figure 12 shows the effect of residual stresses in the bead plate generated during the forming process. The residual stresses were removed after the forming was completed. The residual stresses have beneficial effect when the sealing gap variation is large.

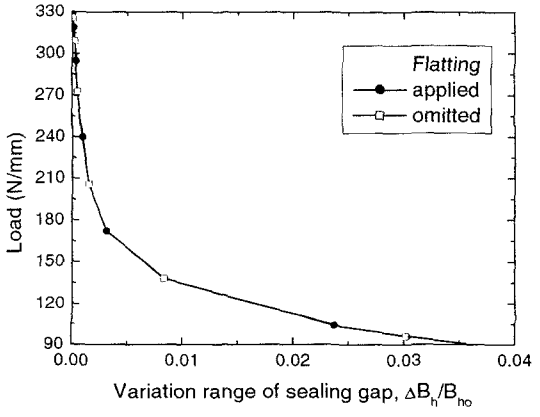

Figure 11. Effect of flatting operation.

All the above results imply that the sealing performance depends not only on the shape of full-bead but also on the forming process. While the larger deformation of bead plate during the forming process improves the sealing performance, it may reduce the fatigue crack resistance because the more strong tensile residual stresses can be generated in the bead plate. Therefore, it is recommended that the present result should be used in the design of the forming process only when the sufficient fatigue crack resistance can be guaranteed. The research on the fatigue crack resistance of full-bead is currently in progress and the result will be presented in the near future.

4. CONCLUSIONS

A finite element model has been developed to simulate the forming process of the full-bead of MLS gasket and then to assess its sealing performance. Reliability of the model was verified experimentally. Parameter study on the forming process was conducted and the following conclusion was obtained.

The sealing performance of the full-bead is enhanced with more severe deformation of the bead plate during the embossing process, i.e., with the increase in the punching depth, the punch height, the punch width and the friction coefficient of the bead plate against the punch and die, and with the decrease in the width of die cavity. Meanwhile, the flatting process has no influence on the sealing performance.

It is noted that the present result should be used with caution because the severe deformation of the bead plate during the forming can produce the strong tensile residual stresses that is detrimental to the fatigue durability of the full-bead.

REFERENCES

Harland, C. Novaria, P. and Robinson, M. (1993). Process and performance of modeling of gasket components. *SAE Paper No.* 930118.

Herbert, C. and Webster, W. (1998). Cylinder head gasket simulation in finite element analysis. *SAE Paper No.* 980843.

Ishigaki, T., Kitagawa, J. and Tanaka, A. (1993). New evaluation method of metal head gasket. *SAE Paper No.* 930122.

Novak, G., Sadowski, M., Widder, E. and Capretta, R. (1998). The role of the stopper in the mechanics of combustion seal. *SAE Paper No.* 980575.

Popielas, F., Chen, C. and Obermaier, S. (2000). CAE approach for multi-layer steel cylinder head gaskets. *SAE Paper No.* 2000-01-1348.

Yamaguchi, K., Sato, A., Goto, E., Fujiki, R., Kawai, Y. and Nakata, N. (1998). Development of a new metal cylinder head gasket. *SAE Paper No.* 980844.